

Synthesis of quantum-confined CdS nanotubes

A. K. Mahapatra*

Institute of Physics, Sachivalaya Marg, Bhubaneswar, 751005, India

CdS nanotubes with wall thickness comparable to excitonic diameter of the bulk material are synthesized by a chemical route. A change in experimental conditions result in formation of nanowires, and well-separated nanoparticles. The diameter and wall thickness of nanotubes measured to be 14.4 ± 6.1 and 4.7 ± 2.2 nm, respectively. A large number of CdS nanocrystallites having wurzite structure constitute these nanotubes. These nanotubes show high energy shifting of optical absorption and photoluminescence peak positions, compared to its bulk value, due to quantum confinement effect. It is proposed that nucleation and growth of bubbles and particles in the chemical reaction, and their kinetics and interactions are responsible for the formation of nanotubes.

PACS numbers: 61.46.+w; 81.10.Dn; 78.55.Et; 78.67.Ch

Introduction

The discovery of carbon nanotubes (Iijima 1991) has generated considerable research interest to synthesize such type of tubular nanostructures of other materials and study its properties. Carbon nanotubes are conceptualized as the wrapping of graphite layers into a seamless cylinder. Synthesis of single crystalline nanotubes of other similar type of layered materials like BN (Chopra et al. 1995), MoS_2 (Feldman et al. 1995) and WS_2 (Tenne et al. 1992) are reported. In these materials, there exists a strong force within the layer plane, but a weak van der waals force between the inter-layer planes. It helps such materials to self assemble in the form of nanotubes. However, comparatively more isotropic materials like CdS (Zhan et al. 2000), CdSe (Duan and Lieber 2000), GaAs (Duan et al. 2000), and Si (Yu et al. 1998) tend to form nanowires instead of nanotubes. Therefore, nanotubes of these isotropic materials are generally synthesized by using nanowires as templates. CdS nanotubes are also synthesized by using Sn nanowires as the template (Hu et al. 2005). However, those synthesized CdS nanotubes have a wall thickness much larger than the excitonic diameter of the bulk CdS (6 nm). Hence, no quantum confinement effects could be observed. Aspect ratio and wall thickness of nanotubes play a major role in its mesoscopic properties (Masale et al. 1992). The quantum confinement effect can be observed if the wall thickness of nanotube is comparable to the excitonic diameter of bulk material. It should be noted that quantum confinement effects are least studied in one-dimensional systems, particularly with tubular structure, as compared to other low-dimensional systems.

The present work reports a single-step chemical process to synthesize micron length CdS nanotubes with wall thickness comparable to the excitonic diameter of the bulk material. A change in experimental condi-

tions result in formation of nanowires, and well separated nanoparticles. A mechanism of formation of the nanotube is described. It is proposed that bubbles are playing the key role in formation of nanotubes. Optical absorption and photoluminescence measurements are carried out in order to study the quantum confinement effect.

Experimental

The precursors used for the synthesis of CdS nanotubes are thiourea (NH_2CSNH_2), Cadmium sulfate ($CdSO_4$), ammonia (NH_3), and poly vinyl alcohol (PVA). 0.01 M aqueous solution of $CdSO_4$ and thiourea are prepared separately. About 5 mL of 3 M aqueous ammonia solution is added through a buret into 20 mL of $CdSO_4$ solution in a slow stirring condition. During addition of ammonia it turns to a turbid white solution and then becomes completely transparent. A total of 15 mL of 4% aqueous solution of PVA (degree of polymerization: 1,700 - 1,800) is added to it. About 20 mL of thiourea solution is then put in the same stirring condition, and left in the ambient condition without any further stirring. After around 10 min the solution becomes pale yellow color, which suggests formation of CdS. After 90 min, carbon coated Cu-grids are dipped into this yellow color solution and held aloft to dry. These dried grids are used for transmission electron microscopy (TEM) analysis. For other experiments nanotubes are collected by centrifugation.

TEM is performed using JEOL-2010 operated at 200 KeV electron beam energy. X-ray diffraction (XRD) was conducted on a philips PW1877 diffractometer using Cu K_α radiation. Optical absorption measurements are carried out by using a dual beam Shimadzu UV-3101 PC spectrophotometer. The photoluminescence (PL) measurements are carried out using 369 nm line from a Oriol Hg/Xe lamp as the source of excitation. Luminescence is detected by a PMT detector attached with Jovin Yvon TRIAX-180 spectrometer. Experiments are carried out in ambient temperature.

*e-mail: amulya@iopb.res.in

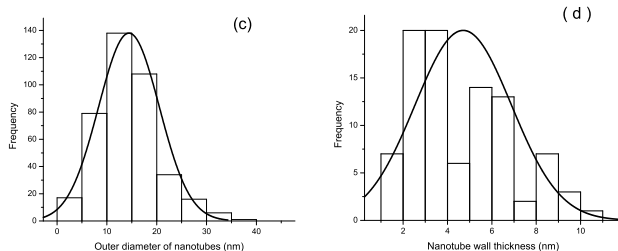
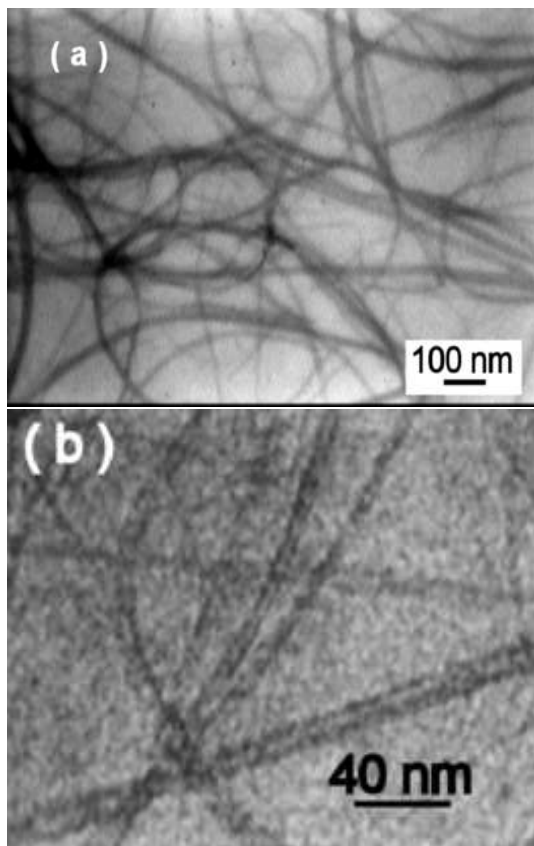


FIG. 1: TEM micro-graphs of CdS nanotubes (a) with lower magnification (b) with higher magnification. (c) Histogram of outer diameter of nanotubes (d) histogram of thickness of nanotubes.

Results and discussions

The formation of CdS nanotubes is confirmed by transmission electron microscopy (TEM). The typical TEM micrographs at a lower and at a higher magnification are shown in Fig.1a, b, respectively. From Fig.1a, it is not possible to conclude whether these are nanotubes or nanowires. However, it is conformed that these nanostructures are of micron lengths and have high aspect ratio. With higher magnification (Fig.1b), a contrast between the solid side wall (darker contrast) and hollow middle part (lighter contrast) of these one-dimensional structure is observed. It gives the signature of forma-

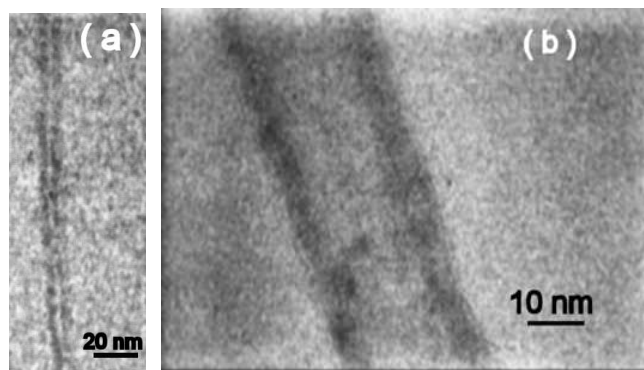
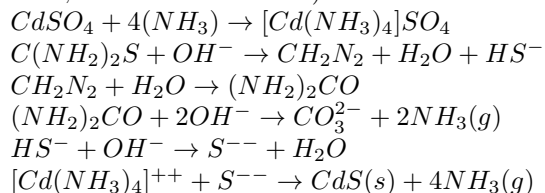


FIG. 2: TEM micro-graphs of (a) a nanotube with smaller diameter (b) a nanotube with bigger diameter.

tion of nanotubes. Outer diameter and wall thickness of several nanotubes are measured. A histogram of outer diameter of CdS nanotubes along with a fitted Gaussian, is shown in Fig. 1c. The mean diameter of the nanotube is 14.4 nm with a standard deviation of 6.1 nm. The histogram of wall thickness, along with a fitted Gaussian, is shown in Fig. 1d. The mean wall thickness of the nanotubes is 4.7 nm with a standard deviation of 2.2 nm. TEM image of a nanotube with a smaller diameter and a nanotube with a larger diameter are shown in Fig. 2 a,b respectively. The fluctuation observed in the thickness of wall is comparatively less than the fluctuation in diameter of the nanotubes.

The electron diffraction (ED) pattern is shown in Fig. 3a. The rings in ED pattern suggests polycrystalline nature of the nanotubes. These nanotubes are not single crystalline, but consists of numerous nanocrystallites as it can be seen in high resolution electron micrograph (Fig.3b). It seems large number of nanocrystallites bind together and form nanotube. X-ray diffraction (Fig. 4) peaks obtained are also broad due to small dimensions of these constituent crystallites. The XRD pattern shows characteristic peaks of wurzite structure of CdS (JCPDS card No. 41-1049). The interplanar distance of 0.24 nm, as shown in Fig.3b, matches for (102) planes and rings in ED pattern corresponds to (110) and (302) planes of wurzite structure of CdS. The formula used to calculate d -value in the ED pattern is $d_{hkl} = \lambda L/R$. where L is the Camera length, R is the radius of the ring and λ is the wavelength of the electron beam.

The general chemical equation for the formation of CdS nanotube can be written as follows (Pavaskar et al. 1977; Hariskos et al. 2001) :



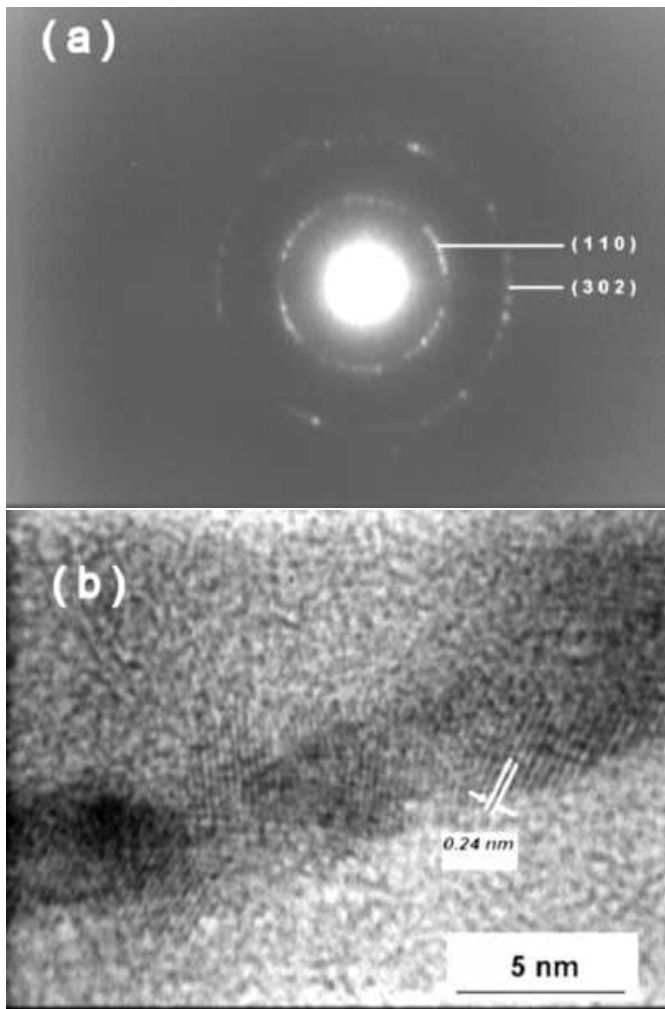


FIG. 3: (a) Diffraction pattern of CdS nanotubes (b) HRTEM micro-graph of a portion of side wall in CdS nanotube.

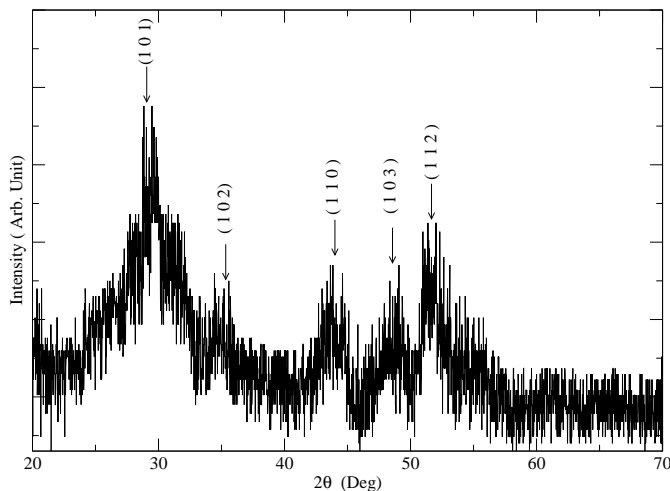


FIG. 4: XRD spectrum of CdS nanotubes.

The chemical reaction mentioned above, leads to supersaturation of CdS concentrations. According to classical nucleation theory (Markov 1995), the energy required to form a critical particle homogeneously is given by:

$$W_p = \frac{1}{3} \sum_n \sigma_n A_n \quad (1)$$

where A_n is surface area and σ_n is specific surface free energy of the n -th surface of the particle. Since crystal faces with different crystallographic orientation have different specific surface energy, the crystallite form a shape in which the total surface energy will be minimum.

It should be noted that the chemical route adopted to synthesize CdS nanotube is similar to the chemical bath deposition technique to make bulk CdS thin films (Pavaskar et al. 1977). The optimization parameters like concentration of the reactant and working temperature are varied. PVA is also used during these chemical synthesis process. PVA is a surface active and water soluble polymer. Although, it does not take part in the chemical reaction, its addition increases viscosity (Briscoe et al. 2000) and decreases surface tension (Bhattacharya and Ray 2004) of the solution.

According to the Henry's law, the amount of a gas dissolved in a given volume of liquid, C_{eq} , is directly proportional to the partial pressure of that gas, P , above the liquid. It can be written as:

$$C_{eq} = kP \quad (2)$$

where k is the Henry's law constant.

As viscosity of the solution is increased due to addition of PVA, the diffusional escape of the ammonia gas decreased and higher concentration of gas generated inside the solution than its equilibrium concentration. It results in supersaturation and nucleation of ammonia gas bubble inside the solution.

The energy required to form a critical bubble homogeneously (Landau and Lifshitz 1999; Bowers et al. 1995) is given by

$$W_b = \frac{1}{3} \sigma A = \frac{16\pi\sigma^3 k^2}{3(C_s - C_{eq})^2} \quad (3)$$

here σ is the surface tension and C_s is the supersaturation concentration.

The probability of formation of critical bubble is proportional to $\exp(-W_b/T)$. Due to presence of σ^3 term in the numerator of W_b , the probability of formation of gas bubbles is increased significantly by the reduction of surface tension.

Although we considered the case of a homogeneous nucleation, the colloids (both bubbles and particles) most likely nucleate heterogeneously, as later process is energetically favorable than the former.

These colloids experience the gravitational forces due to its mass, the buoyant force due to the displaced fluid

and the frictional force due to viscosity of the medium. This leads to a terminal velocity at which these colloids will move and is given by the equation (Lamb 1945)

$$V = \frac{2}{3} \cdot \frac{gr^2(\rho' - \rho)}{\eta} \cdot \frac{\eta + \eta'}{2\eta + 3\eta'} \quad (4)$$

Here ρ' and η' are the density and dynamic viscosity of the colloids, respectively. Similarly ρ and η are the density and dynamic viscosity of the medium, respectively. g is the acceleration due to gravity and r is the radius of the colloids. For particles, we can approximate $\eta' \gg \eta$; and for bubbles, $\eta' = 0$ and $\rho' = 0$. Hence, according to the above equation, the terminal velocity of colloids with size in nano range have a negligibly small terminal velocity. These colloids also experience a random force that originates from fast collisions with molecules of the medium. This gives rise to Brownian motion of the colloids. The average squared displacement of the colloid, $\langle x^2 \rangle$, that follows Brownian motion, after time t from its initial position is given by (Reif 1965)

$$\langle x^2 \rangle = \left(\frac{k_B T}{3\pi\eta r} \right) t \quad (5)$$

The average squared displacement is inversely proportional to the radius of the colloid and to the viscosity of the medium. Hence, diffusive motion dominates the motion of the particles and bubbles. These particles and bubbles encounter during their random motion inside the solution, and during this process, the particles get attached with the bubbles. It should be noted that particle-bubble attachment can occur when particle-bubble contact time is longer than the induction time (Dai et al. 1999). Hence, reduction in induction time enhance the attachment efficiency. As bubbles and particles are very small in size, the induction time is very small and attachment efficiency is very high. The induction time is defined as the time for the liquid film between the particle and the bubble to thin, rupture and form a equilibrium three-phase contact.

It is observed that CdTe nanoparticles spontaneously aggregate into a pearl-necklace like structure upon controlled removal of the protective shell of organic stabilizer, and subsequently recrystallize into nanowires (Tang et al. 2002). These CdTe nanoparticles have a large dipole moment and the dipole-dipole interaction between them is responsible for their unidirectional self-organization (Sinyagin et al. 2005). CdS nanoparticles with wurzite crystal structure also have a large dipole moment (Sinyagin et al. 2005; Blanton et al. 1997; Shanbhag and Kotov 2006). Hence, particle-attached-bubble as a whole may has a strong net dipole moment; and dipole-dipole interaction between these particle-attached-bubbles is primarily responsible for their unidirectional aggregation. The adjacent nanoparticles on the bubble surface probably get attached at a planar interface, reduce total surface energy and transform into a

stable nanotube. In the aggregation-based crystal growth (Banfield et al. 2000; Penn and Banfield 1998), random force imparted on the nanoparticles by the medium molecules helps them in rotation and attachment at a planar interface so that they can share a common crystallographic orientation. However, even a small misorientation can lead to dislocation at the interfaces. As the medium is viscous and CdS nanoparticles are attached on a curved surface with equilibrium three phase contact, particles could not perfectly orient and attach in a atomically flat interfaces to give a dislocation free single crystalline nanotube. However, annealing after synthesis can help in improving the crystallinity.

It should be noted that colloids after nucleation goes through subsequent growth dynamics along with the above mention steps like bubble-particle attachment and unidirectional aggregation of particle-attached-bubbles. The colloids smaller than its critical size dissolve as surface energy is large. Colloids bigger than the critical size only grow. The attachment of colloids also reduces the total surface energy and effective size of the colloid become more than its critical radius. Hence, formation of nanotubes with a high aspect ratio are favorable and stable. In the TEM measurement, it is observed that inner wall of nanotubes are comparatively less smooth than the outside wall. A TEM micrograph of a nanotube in a formative stage, in which bubbles are coalescing, is shown in figure (Fig.5a). Other possible nanostructures like nanoparticles, nanowires, nanowires with spherical cavity(Fig.5b) are also observed in TEM measurements, although they are few in number. These observations lead to believe that bubbles are responsible for hollowness inside the nanotube.

In order to confirm the role of PVA, experiments are carried out in similar experimental condition by not using PVA, and by using much higher amount of PVA (25 mL of 20% aqueous solution). Nanowires are seen in TEM measurements instead of nanotubes, when PVA is not used in the experiment. The typical TEM micrographs at a lower and at a higher magnification are shown in Fig.6a,b respectively. In this case probably bubbles did not nucleate. Nanoparticles get aligned unidirectionally due to their dipole moment and nanowires are formed. Formation of nanowires even in the absence of PVA exclude the possibility that linear chain structure of polymer is somehow acting as a template for unidirectional aggregation of the nanoparticles, and forming nanotubes.

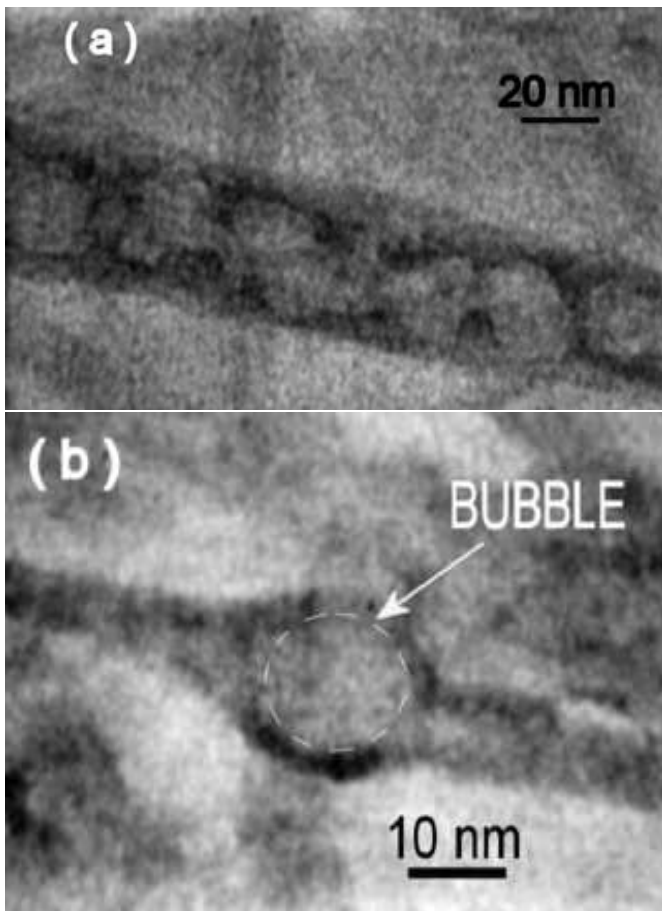


FIG. 5: TEM micrographs of (a) a nanotube in the formative stage (b) a nanowire with a rounded bulge.

When excess amount of PVA is used, the solution becomes very viscous. Only after ≈ 4 h (in contrast to ≈ 10 min), the solution becomes pale yellow color. The solution then kept for another 90 min, and then spin-coated on a Cu-grid to carry out TEM measurements. Even though TEM is carried out by taking the grid on a liquid nitrogen cooled sample stage, the PVA matrix forms voids due to the heating effect of electron beams. However, it can be seen that nanocrystals are well separated. With too much increase in viscosity, the decrease in diffusive length of nanocrystals is significant (see Eq. 5). So nanocrystals could not aggregate to form nanowires or nanotubes. A typical TEM micrograph is shown in Fig. 7. It should be noted that well separated HgS nanocrystals are also synthesized by a similar chemical procedure using PVA (Mahapatra and Dash 2006).

Most of the interesting properties exhibited by semi-conducting nanomaterials are attributed to quantum confinement effect. The electronic energy levels are strongly dependent on the size and also on the shape of the nanostructure (Kayanuma 1991). In the one-dimensional systems charge carriers are confined in two

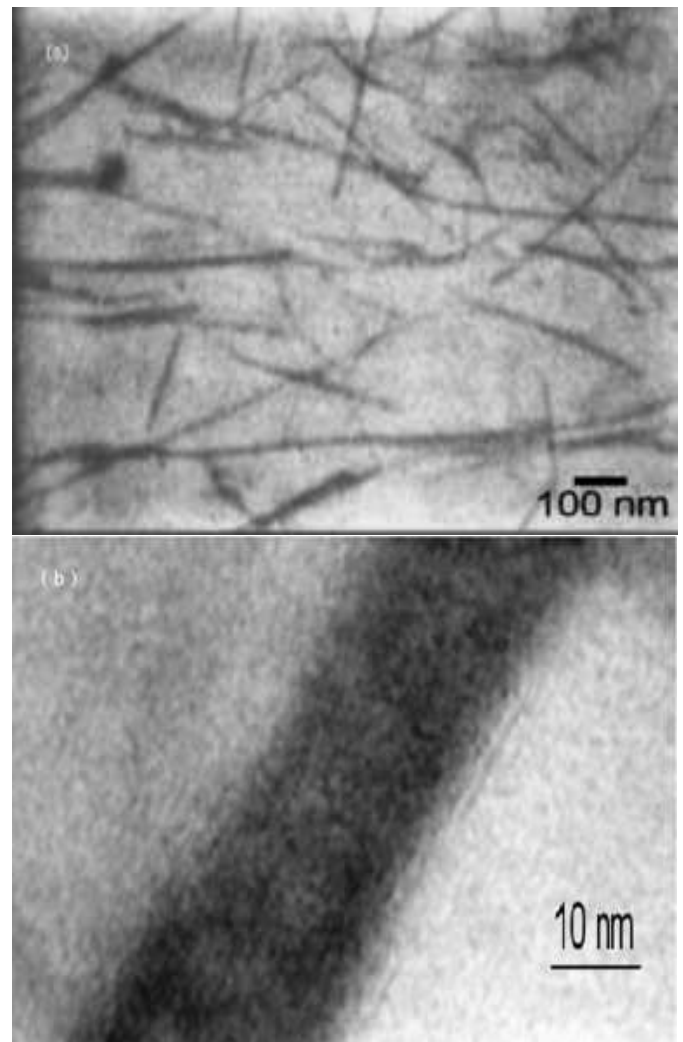


FIG. 6: TEM micro-graphs of (a) CdS nanowire with lower magnification, and (b) a single nanowire with higher magnification.

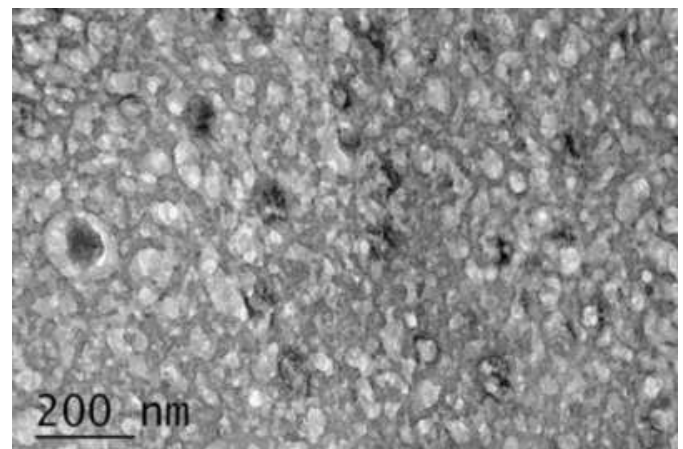


FIG. 7: TEM micro-graph of CdS nanocrystals.

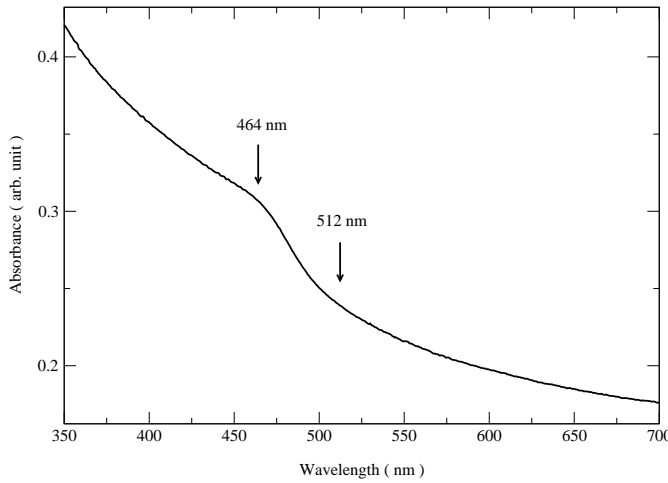


FIG. 8: Optical absorption spectrum of CdS nanotubes.

dimensions and free in one dimension. The spatial confinement of carriers leads to band gap widening and most directly realized by a high energy shift in optical absorption and photoluminescence peak. Quantum confinement effect for zero-dimensional system is studied both theoretically (Kayanuma 1988) and experimentally (Vossmeier et al. 1994) in detail. However, it is not well understood for one-dimensional systems, particularly with tubular structure.

The optical absorption spectrum and photoluminescence (PL) spectrum of CdS nanotubes are shown in Figs. 8, 9, respectively. An excitonic peak appears at 464 nm in the optical absorption spectrum. The peak position is blue shifted by 48 nm from its bulk band gap value (512 nm). The experimental PL data is fitted as the sum of two Gaussian functions, among which one is due to incident line. The PL peak is best fitted with the Gaussian of 492 nm mean and 26 nm standard deviation. It should be noted that, the PL peak position is also blue shifted from its bulk band gap value. High energy peak shifting in the optical absorption and PL spectra are expected due to quantum confinement effect as nanotube wall thickness is comparable to excitonic diameter of bulk CdS.

Luminescence that are observed in semiconductor nanomaterials are generally excitonic and trapped emissions. Excitonic emission is sharp and can be observed near the absorption edge if the material is pure (Pankove 1975). However, if the material is impure or off-stoichiometric then a broad and intense emission occur at higher wavelength due to recombination of charge carriers at trapped states. Hence the band edge luminescence that appears at 492 nm is due to excitonic transition. Band edge luminescence at 470 nm is also observed for CdS nanotubes synthesized by sacrificial template method (Li et al. 2006). However, CdS nanotubes

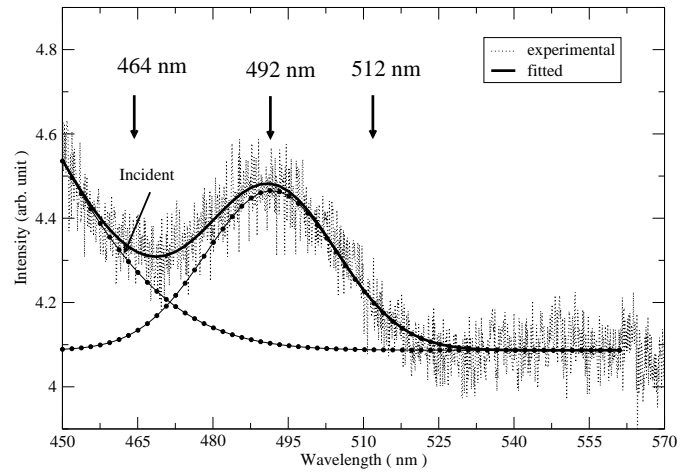


FIG. 9: Photoluminescence spectrum of CdS nanotubes. Experimental data is fitted with Gaussian functions.

synthesized by sacrificial template method also show a very intense and broad peak centered around 560 nm due to presence of trapped states. No such peak is observed in our synthesized CdS nanotubes. This suggests purity and stoichiometric nature of our synthesized CdS nanotubes.

Excitonic transition in a semiconductor can be observed well only at low temperature. However, it can be observed even at room temperature due to enhancement of oscillator strength in the low-dimensional systems (Kayanuma 1991). It should be noted that excitonic transitions is not observed in optical absorption and PL measurements for bulk CdS which was prepared by the similar chemical route (Pavaskar et al. 1977). However, a clear excitonic feature arises in both absorption and PL measurements when it forms nanotubes. The PL peak is red shifted by 150 meV with respect to absorption peak. Such a large red shift, known as stokes shift, of 147 meV is also reported for CdS nanoparticles (Tamborra et al. 2004). The difference in the absorption and emission states avoid sample self-absorption and could be very useful in making LEDs (Sze 1981).

Conclusion

CdS nanotubes with wall thickness comparable to excitonic diameter of the bulk material are synthesized by a chemical synthesis process. These synthesized nanotubes show band gap widening and enhanced oscillator strength due to quantum confinement effects. A large stokes shift of 150 meV is also observed. Bubbles are responsible for the hollowness of nanotubes; and bubbles of dissolved gases can be utilized to make nanostructures with hollow interior.

Acknowledgment

The help and encouragement received from Dr S. N. Sahu is gratefully acknowledged. Mr A. K. Dash, Mr U. M. Bhatta, and Dr P. V. Satyam are acknowledged for their help in TEM measurements.

-
- [1] Banfield JF, Welch SA, Zhang H, Ebert TT, Penn RL (2000) Aggregation-based crystal growth and microstructure development in natural iron oxyhydroxide biomineralization products. *Science* 289:751-754
- [2] Bhattacharya A, Ray P (2004) Studies on surface tension of poly(vinyl alcohol): effect of concentration, temperature, and addition of chaotropic agents. *J Appl Polym Sci* 93:122-130
- [3] Blanton SA, Leheny RL, Hines MA, Sionnest PG (1997) Dielectric dispersion measurements of CdSe nanocrystal colloids: Observation of a permanent dipole moment. *Phys Rev Lett* 79:865-868
- [4] Bowers PG, Hofstetter C, Letter CR, Toomey RT (1995) Supersaturation limit for homogeneous nucleation of oxygen bubbles in water at elevated pressure: "superhenry's law". *J Phys Chem* 99:9632-9637
- [5] Briscoe B, Luckham P, Zhu S (2000) The effects of hydrogen bonding upon the viscosity of aqueous poly(vinyl alcohol) solution. *Polymer* 41:3851-3860
- [6] Chopra NG, Luyken RJ, Cherrey K, Crespi VH, Cohen ML, Louie SG, Zettl A (1995) Boron nitride nanotubes. *Science* 269:966-967
- [7] Dai Z, Fornasiero D, Ralston J (1999) Particle-bubble attachment in mineral flotation. *J Colloid Interface Sci* 217:70-76
- [8] Duan X, Lieber CM (2000) General synthesis of compound semiconductor nanowires. *Adv Mater* 12:298-302
- [9] Duan X, Wang J, Lieber CM (2000) Synthesis and optical properties of gallium arsenide nanowires. *Appl Phys Lett* 76: 1116-1118
- [10] Feldman Y, Wasserman E, Srolovitz DJ, Tenne R (1995) High-rate, gas-phase growth of MoS_2 nested inorganic fullerenes and nanotubes. *Science* 267: 222-225
- [11] Hariskos D, Powalla M, Chevaldonnet N, Lincot D, Schindler A, Dimmler B (2001) Chemical bath deposition of CdS buffer layer: prospects of increasing materials yield and reducing waste. *Thin Solid Films* 387: 179-181
- [12] Hu JQ, Bando Y, Zhan JH, Liao MY, Golberg D, Yuan XL, Sekinuchi T (2005) Single-crystalline nanotubes of IIB-VI semiconductors. *Appl Phys Lett* 87: 113107
- [13] Iijima (1991) Helical microtubules of graphitic carbon. *Nature* 354: 56-58
- [14] Kayanuma Y (1988) Quantum-size effects of interacting electrons and holes in semiconductor microcrystals with spherical shape. *Phys Rev B* 38: 9797-9805
- [15] Kayanuma Y (1991) Wannier excitons in low-dimensional microstructures: shape dependence of quantum size effect. *Phys Rev B* 44: 13085-13088
- [16] Lamb H (1945) *Hydrodynamics*, 6th edn. Dover, New York
- [17] Landau LD, Lifshitz EM (1999) *Statistical physics*, 3rd edn. Butterworth Heinemann
- [18] Li X, Chu H, Li Y (2006) Sacrificial template growth of CdS nanotubes from $Cd(OH)_2$ nanowires. *J Solid State Chem* 179:96-102
- [19] Mahapatra AK, Dash AK (2006) α -HgS nanocrystals: synthesis, structure and optical properties. *Physica E* 35: 9-15
- [20] Markov IV (1995) *Crystal growth for beginners*, World scientific
- [21] Masale M, Constantinou NC, Tilley DR (1992) Single-electron energy subbands of a hollow cylinder in an axial magnetic field. *Phys Rev B* 46: 15432-15437
- [22] Pankove JI (1975) *Optical process in semiconductors*, Dover Publications Inc., N.Y.
- [23] Pavaskar NR, Menezes CA, Sinha APB (1977) Photoconductive CdS films by a chemical bath deposition process. *J Electrochem Soc* 124: 743-748
- [24] Penn RL, Banfield JF (1998) Imperfect oriented attachment: dislocation generation in defect-free nanocrystals. *Science* 281: 969-971
- [25] Reif F (1965) *Fundamentals of statistical and thermal physics*, McGraw-Hill, New York
- [26] Shanbhag S, Kotov NA (2006) On the origin of a permanent dipole moment in nanocrystals with a cubic crystal lattice: effects of truncation, stabilizers, and medium for CdS tetrahedral homologues. *J Phys Chem B* 110:12211-12217
- [27] Sinyagin A, Belov A, Kotov N (2005) Monte Carlo simulation of linear aggregate formation from CdTe nanoparticles. *Model Simul Mater Sci Eng* 13:389-399
- [28] Sze SM (1981) *Physics of semiconductor devices*, Wiley Interscience
- [29] Tamborra M, Striccoli M, Comparelli R, Curri ML, Petrella A, Agostiano A (2004) Optical properties of hybrid composites based on highly luminescent CdS nanocrystals in polymer. *Nanotechnology* 15:S240-S244
- [30] Tang Z, Kotov NA, Giersig M (2002) Spontaneous organization of single CdTe nanoparticles into luminescent nanowires. *Science* 297:237-240
- [31] Tenne R, Margulis L, Genut M, Hodes G (1992) Polyhedral and cylindrical structures of tungsten disulfide. *Nature* 360:444-446
- [32] Vossmeier T, Katshikas L, Giersig M, Popovic IG, Weller H (1994) CdS nanoclusters: synthesis, characterization, size dependent oscillator strength, temperature shift of the excitonic transition energy, and reversible absorbance shift. *J Phys Chem* 98:7665-7673
- [33] Yu DP, Bai ZG, Ding Y, Hang QL, Zhang HZ, Wang JJ, Zou YH, Qian W, Xiong GC, Zhou HT, Feng SQ (1998) Nanoscale silicon wires synthesized using simple physical evaporation. *Appl Phys Lett* 72:3458-3460
- [34] Zhan J, Yang X, Wang D, Li S, Xie Y, Xia Y, Qian Y (2000) Polymer-controlled growth of CdS nanowires. *Adv Mater* 12:1348-1351